Journal of
Polymer Materials

Tech Science Press

http://doi.org/10.32604/jpm.2026.088128

ARTICLE

Tamarindus Indica Bark Powder as a Sustainable Bio-Based Filler for Enhancing Bondline Uniformity and Performance of Polyurethane Adhesives in Wood Bonding

Lakshmana Rao Bhagavathi[1,*], Sk. Gouse[1], T. Siva[2] and Mohammad Faseeulla Khan[3,*]

[1]Department of Mechanical Engineering, Rajiv Gandhi University of Knowledge Technologies Nuzvid, Eluru District, India
[2]Department of Metallurgical & Materials Engineering, Rajiv Gandhi University of Knowledge Technologies Nuzvid, Eluru District, India
[3]Department of Mechanical Engineering, College of Engineering, King Faisal University, Al-Ahsa, Saudi Arabia
*Corresponding Authors: Lakshmana Rao Bhagavathi. Email: lakshman@rguktn.ac.in; Mohammad Faseeulla Khan. Email: fmohammad@kfu.edu.sa

Received: 29 June 2026; Accepted: 14 September 2026; Published: 24 September 2026

ABSTRACT: Polyurethane (PU) adhesives are extensively used in wood bonding due to their high reactivity and strong adhesion. However, excessive penetration of the adhesive into the wood substrate often results in non-uniform bondline thickness, which can compromise joint performance. The use of environmentally compatible fillers offers a sustainable approach to address this limitation. In the present study, Tamarindus indica bark powder was used as a natural filler to achieve uniform bondline thickness in PU-bonded joints. Lap-shear joints were produced using untreated and treated bark powders at varying weight fractions, reinforced within a one-component moisture-curing PU adhesive. The mechanical performance and bondline morphology of these joints were systematically evaluated and compared with PU joints reinforced with microcrystalline cellulose. Further, Fourier transform infrared (FTIR) spectroscopy and thermogravimetric analysis (TGA) of all the samples were performed. Results indicate that the addition of bark powder enhances bondline uniformity, improves lap-shear strength, and increases thermal stability compared to unreinforced PU samples. The results demonstrate that Tamarindus indica bark powder can effectively enhance bondline uniformity, mechanical strength, and thermal stability, establishing it as a viable bio-based reinforcement for advanced PU adhesive systems in wood bonding applications.

KEYWORDS: Polyurethane adhesives; wood bonding; bondline thickness; Tamarindus indica bark powder; green fillers; microcrystalline cellulose

1 Introduction

PU adhesives are widely employed across diverse industries due to their strong adhesion and versatile bonding capabilities. In the automotive sector, they are used for joining metal-to-metal, metal-to-glass, and fiber-reinforced polymer (FRP) components. In wood bonding, PU adhesives are particularly valued for their high reactivity with hydroxyl-rich components of wood such as cellulose, lignin, and hemicellulose. These functional groups readily react with isocyanates to form durable polyurethane linkages. Despite their effectiveness, a persistent challenge in wood bonding is achieving uniform bondline thickness. Excessive penetration of isocyanates into the porous wood structure often leads to non-uniform bondlines, which can compromise joint strength and reliability. One promising strategy to mitigate this issue is the use of compatible fillers that regulate adhesive penetration and improve bondline morphology.

Raw bark is increasingly being explored as a sustainable filler for wood adhesive systems due to its rich content of extractives, such as tannins and polyphenols, which can actively influence adhesive performance. Unlike conventional inert fillers, these acidic extractives may modify the bond line pH and affect the curing behaviour of moisture-curing one-component polyurethane (1K PUR) adhesives. By influencing the balance between gelling and blowing reactions during curing, bark extractives can contribute to improved cross-linking, reduced void formation, and enhanced bond line integrity. Therefore, understanding the role of bark extractives and their effect on bond line pH is important for optimizing curing kinetics and improving the mechanical performance of polyurethane-bonded joints.

Extensive research has explored the reinforcement of PU matrices with cellulosic fibers and fillers to enhance mechanical and thermal properties. Otto et al. investigated lignocellulosic fiber-reinforced PU hybrid composites using sugarcane, rice husk, and sisal fibers [1]. They reported superior mechanical performance in terms of elastic modulus, compressive strength and resilience in sugarcane and rice husk composites compared to sisal, attributing the difference to better fiber dispersion and adhesion. Wu et al. demonstrated that microcrystalline cellulose dispersed in PU matrices forms covalent bonds with isocyanates, resulting in nanocomposites with high tensile strength and elongation [2]. Similarly, Rueda et al. modified cellulose nanocrystals with hexamethylene diisocyanate, confirming strong physical association with PU hard domains [3]. Lee et al. synthesized nanofibril-reinforced PU composites via *in-situ* polymerization, showing significant improvements in tensile strength, toughness, and thermal stability [4]. Saralegi et al. examined bio-based PU systems with varying hard segment content and found that cellulose nanocrystals interacted with disordered regions, though mechanical improvements were limited [5].

Weaver and Owen confirmed through infrared spectroscopy that isocyanates react rapidly with moisture and lignin in wood, faster than with cellulose alone [6]. Chen and Yan similarly observed that moisture accelerates curing reactions in pMDI adhesives across different wood species [7]. Pommier and Elbez reported superior bondline continuity in wet wood joints compared to dry ones, highlighting the importance of adhesive penetration control [8]. These studies combinedly establish that cellulosic fillers can react with isocyanates, improving mechanical properties and influencing bondline morphology.

Beyond cellulose, lignin and bark-derived fillers have attracted attention for their compatibility with PU adhesives. García et al. demonstrated that lignin reinforcement reduced adhesive penetration and improved aging resistance due to lignin's hydrophobicity [9]. Chen and Yan used Western red cedar bark particles in pMDI adhesives, showing that moist bark reacted more rapidly with isocyanates than oven-dried bark, thereby improving bondline thickness [7]. Chen et al. further reinforced pMDI adhesives with lignin-containing cellulose nanofibrils, achieving continuous bondlines and confirming PU linkage formation [10]. These findings highlight the potential of bark-derived fillers to regulate adhesive penetration and enhance joint durability.

Sharma et al. reviewed commercial applications of cellulosic nanocomposites, emphasizing extraction, surface modification, and reinforcement strategies [11]. Bhagavathi et al. studied microcrystalline cellulose and hardwood sawdust in moisture-curing PU adhesives, reporting faster curing and improved mechanical properties [12]. In a subsequent study, they demonstrated enhanced long-term durability and hygrothermal resistance in cellulosic-reinforced PU joints compared to saw-dust-reinforced systems. Gadhave et al. partially replaced polypropylene glycol with kraft lignin in PU adhesives, finding improved shear strength but slower setting times due to reduced free isocyanate content [13].

Bark, often considered a low-value byproduct, contains polyphenolic and cellulosic molecules that can be transformed into high-value materials. Ajao et al. demonstrated bark-derived prototypes for PU foams and polypropylene composites, showing competitive mechanical and thermal properties relative to

fossil-based equivalents [14]. Jin et al. analysed red oak and yellow poplar bark, sapwood, and heartwood, confirming lignin's high char yield compared to cellulose and xylan [15]. These studies suggest that bark is a promising source of functional fillers for polymer systems, offering both performance and sustainability benefits.

Recent work has also focused on bio-based PU adhesives. Tenorio-Alfonso et al. compared solvent-based and solvent-free synthesis routes using cellulose acetate, hexamethylene diisocyanate, and castor oil, demonstrating improved curing time, thermal stability, and modulus [16]. Kawalerczyk et al. reinforced urea-formaldehyde adhesives with micro- and nanocellulose, enhancing viscosity, curing behaviour, and bonding quality. Sozen et al. studied polypropylene composites with wood flour and cellulose fibers, reporting improved flexural strength and modulus [17]. Krishnamurthi et al. examined wood flour micro-fillers in PU foams, noting increased density and strength in flexible foams but reduced properties in rigid foams [18]. Pereira et al. developed bio-based PU wood adhesives by synthesizing polyols directly from impurified cashew nutshell liquid through epoxidation and ring-opening reactions with ethanol and ethylene glycol [19]. Natural gums are widely used in food packaging because they are cheap, thicken easily, and stabilize emulsions well. Spinning them into electro spun nanofibers makes them even better, giving the material a higher surface area, better porosity, and greater mechanical strength than standard bulk gum [20]. Poor dispersion of raw cellulose in PLA matrices has traditionally limited composite performance. Using a rosin emulsion to treat microcrystalline cellulose offers a greener, scalable fix—enabling straightforward twin-screw processing and yielding composites with much better stress transfer and durability [21]. The wood composite sector is actively moving away from traditional formaldehyde-based glues due to toxicity and reliance on petrochemicals. Recent literature emphasizes developing robust green adhesives from natural polymers and plant oils that match industrial performance standards [22]. Researchers prepared polyurethane-modified epoxy through a direct, single-step reaction without prepolymers, evaluating reaction times longer reaction periods promoted greater molecular weight and polymer reactivity, leading to measurable gains in tensile strength, viscosity, and pot life over neat epoxy systems [23]. These studies highlight the broad applicability of natural fillers in adhesive and composite systems.

While significant progress has been made in incorporating cellulose and lignin fillers into PU adhesives, limited attention has been given to bark-derived fillers for controlling bondline thickness in hardwood bonding. The present study addresses this gap by investigating the effect of lignocellulosic fillers, specifically Tamarindus indica bark powder and microcrystalline cellulose, on the performance of one-component moisture-curing PU adhesives used for bonding Mangifera indica hardwood. The study systematically evaluates filler–adhesive interactions using FTIR and assesses lap-shear strength and thermal stability through TGA at varying filler weight fractions. By exploring bark-derived fillers as sustainable reinforcements, this work aims to advance eco-friendly adhesive formulations with improved bondline uniformity, mechanical reliability, and thermal stability.

2 Materials and Methods

2.1 Materials

A one component moisture curing PU adhesive (1K PUR, Fevicol, India) was used for all bonding experiments. Mangifera indica hardwood was selected as the substrate material. Microcrystalline cellulose (MCC) was used as a reference filler, whereas bark powder derived from Tamarindus indica was processed and tested as the experimental filler.

2.2 Preparation of Bark Powder and Lignocellulose

Fresh bark from Tamarindus indica trees was collected, chopped into small pieces, and dried. The dried bark was ground using a cross-beater mill and sieved with Kelson's testing equipment to obtain particles of approximately 106 μm (ISS standard sieve size). For lignocellulose extraction, bark powder was dried at 105°C for 3 h in a hot air oven. The powder was then mixed with an aqueous solution containing 3% sodium sulphite at a ratio of 1:7 (w/v). The mixture was heated at 90°C for 3 h under reflux condenser [24]. The resulting suspension was filtered, washed, and dried to obtain lignocellulose powder.

2.3 Substrate Preparation

Rectangular specimens of Mangifera indica wood (101.6 mm × 25 mm × 5 mm) were cut for lap shear testing using a combined planer cutting machine. Prior to bonding, the wood surfaces were abraded with P220 grit emery paper to achieve an average surface roughness of Ra ≈ 1.4 μm, measured using a surface roughness meter. The samples were dried to reduce the moisture content below 10% and verified with an ACETEQ digital wood moisture meter. The substrates were ultrasonically cleaned in acetone for 20 min and air-dried.

2.4 Bonding Procedure

Fillers (MCC, untreated bark powder (UT), and lignocellulose (T)) were preheated at 103 ± 2°C for 3 h to remove residual moisture. Adhesive formulations were prepared by mixing PU adhesive with varying weight fractions of fillers. The mixtures were placed in a desiccator for 3 min to eliminate entrapped air bubbles. The adhesive was applied at a spread rate of 0.03 mL/cm^2, corresponding to an adhesive loading of 36 mg/cm^2. The total adhesive mass was adjusted to account for the different filler loading levels incorporated into each formulation while maintaining a consistent application rate across all samples. Bonded joints were fabricated with an overlap length of 25 mm and a bond line thickness of 0.3 mm maintained using spacers. Bond and grip areas were marked prior to adhesive application. Joints were prepared according to ASTM D906 standards (Fig. 1a) and a sample joint after bonding is shown in Fig. 1b [25–27]. Bonding was performed under controlled laboratory conditions (25 ± 2°C, 50% ± 5% relative humidity) in batches of 5 using a dedicated metal fixture maintained at a uniform pressure of 15 bar. All joints were cured for seven days before further characterization and mechanical testing.

2.5 Characterization of the Bonded Joints

Samples are prepared with different compositions of reinforcements and all the sample conditions with designations are summarized in Table 1. Lap-shear strength was evaluated using a Zwick Roell Z100 universal testing machine. A crosshead speed of 13 mm/min was maintained during testing. At least five specimens per each condition were tested, and average values with standard deviations were reported.

The particle size and morphology of MCC and untreated bark powders were analysed using scanning electron microscopy (SEM, TESCAN VEGA 3SBH). The mean particle size was measured at 23.78 μm for MCC, 98.53 μm for raw bark powder, and 88.85 μm for the treated bark powder.

Thermal stability of the adhesives was evaluated using a Setaram Labsys Evo thermogravimetric analyser. Samples were heated from room temperature to 600°C at a rate of 10°C/min under an argon atmosphere. Derivative thermogravimetric (DTG) curves were also obtained to identify decomposition stages.

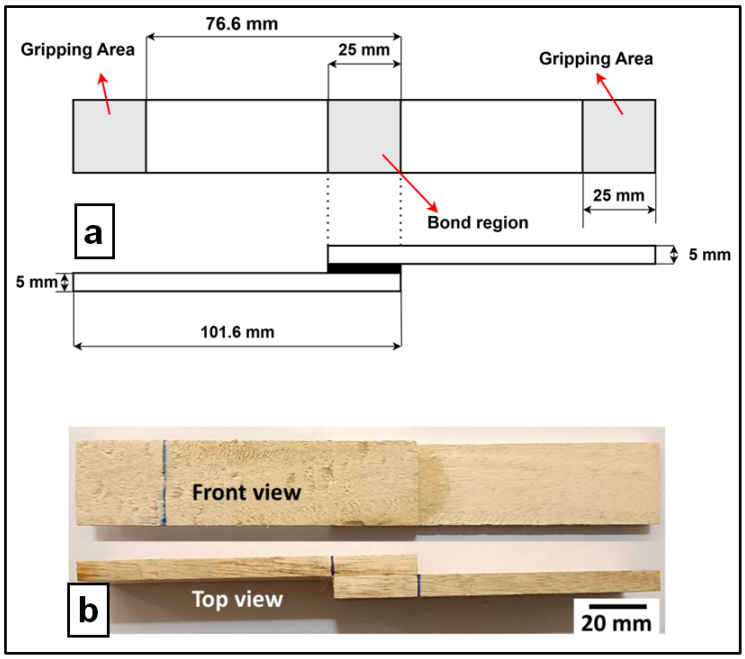

Figure 1: (**a**) Front and top view schematics of lap-shear joint and (**b**) joint after bonding.

Table 1: Samples prepared with different compositions of reinforcement and their designation.

Type of Reinforcement in PU Adhesive	Wt% Range	Sample Codes
Microcrystalline cellulose (MCC)	0.5–5	PU+0.5M, PU+1M, PU+1.5M, PU+2M, PU+2.5M, PU+3M, PU+4M, PU+5M
Untreated bark powder (UT)	0.5–5	PU+0.5UT, PU+1UT, PU+1.5UT, PU+2UT, PU+2.5UT, PU+3UT, PU+4UT, PU+5UT
Treated bark powder (T)	0.5–5	PU+0.5T, PU+1T, PU+1.5T, PU+2T, PU+2.5T, PU+3T, PU+4T, PU+5T
Unreinforced	No filler	PU

Attenuated total reflectance FTIR spectroscopy was performed using a Cary 630 FTIR spectrometer equipped with a multi reflection ZnSe ATR system. Spectra of PU adhesives with and without fillers were collected in the range of 400–4000 cm^{-1} at a resolution of 4 cm^{-1}. FTIR analysis was used to confirm chemical interactions between isocyanate groups and hydroxyl functionalities of the fillers.

Fractured surfaces of lap shear specimens were examined under scanning electron microscope (SEM, TESCAN VEGA 3SBH, accelerating voltage 3 kV). Microstructural features such as filler dispersion, bondline continuity, and failure modes were analysed to correlate with mechanical performance.

3 Results and Discussion

3.1 Bondline Study

SEM image of unreinforced PU joint is shown in Fig. 2, where non-uniform bondline thickness and excessive adhesive penetration into the substrate has been observed. In contrast, SEM images of PU joints reinforced with untreated bark powder (PU+UT) and treated lignocellulose (PU+T), as shown in Fig. 3, reveal distinct improvements in bondline morphology. The PU+UT and PU+T joints exhibit a notably

more consistent bondline across the adhesive–substrate interface, indicating enhanced filler distribution and interfacial contact. The average bondline thickness across all lap-shear joints was approximately 300–400 μm, significantly more uniform than that observed in unreinforced PU joints. Adhesive penetration into the substrate was approximately 10% (30 μm) for neat PU, compared to 5% (15 μm) for the filled PU at different regions. Filler reinforcement not only improved bondline uniformity but also mitigated the issue of excessive adhesive penetration.

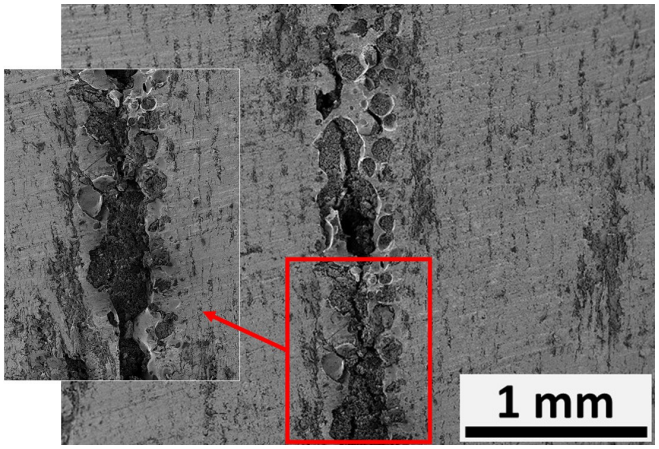

Figure 2: SEM micrograph showing bondline of PU adhesive joint.

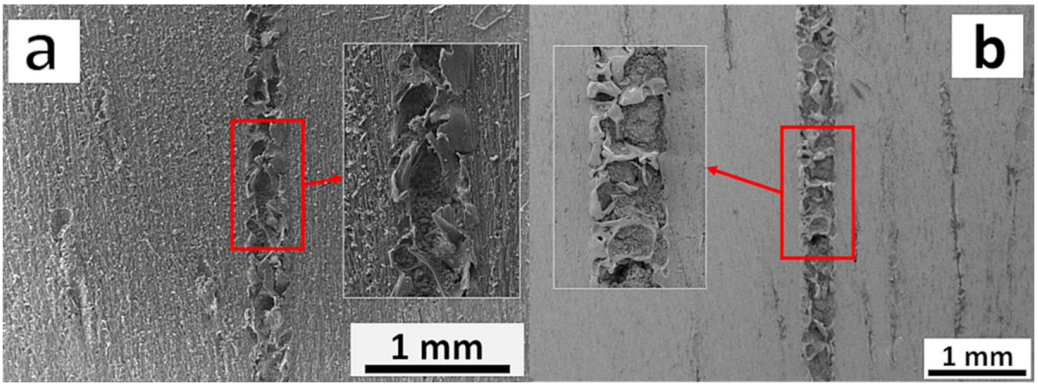

Figure 3: SEM micrographs showing bondline of (**a**) PU+UT and (**b**) PU+T joints.

SEM imaging across multiple regions revealed substantial PU penetration in the neat (plain) samples compared to those containing fillers. As shown in Figs. 4 and 5, higher filler content noticeably reduced penetration; the fillers reacted with the polyurethane matrix to form a restrictive barrier layer that effectively suppressed the crack propagation observed in neat PU. At low magnification both filler adhesive formulations demonstrated structural integrity, forming a continuous and uniform bond line along the substrate interface without detectable macro-scale debonding or linear discontinuities. Elevated magnification images demonstrated strong interfacial bonding between the adhesive and substrate in both cases. Conversely, as shown in Fig. 2, the unmodified PU matrix exhibited crack initiation and structural disruptions stemming from adhesive penetration into the substrate.

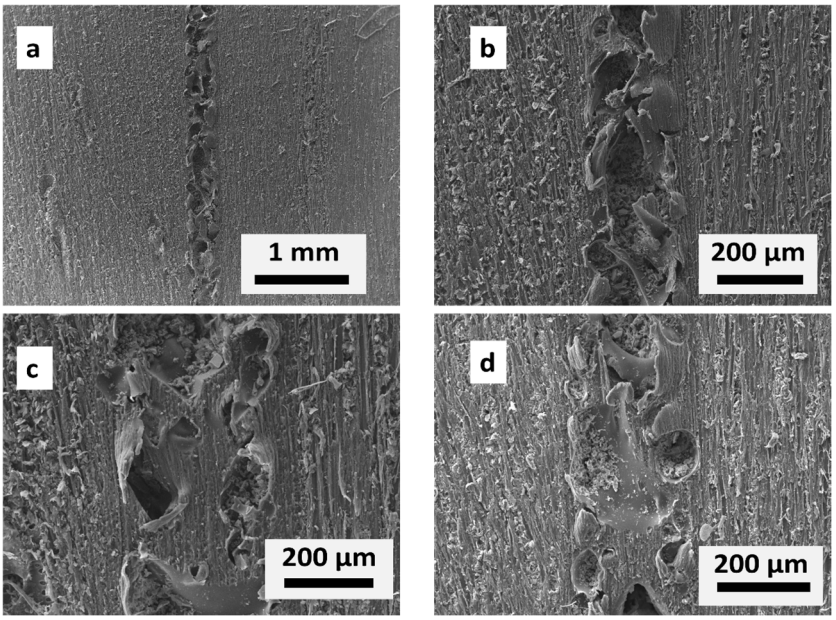

Figure 4: SEM micrographs showing bondline of PU+UT.

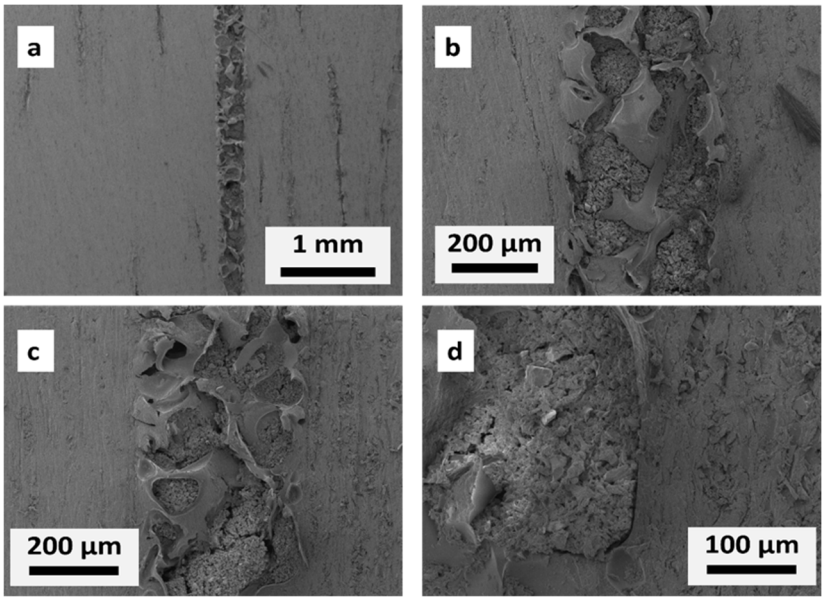

Figure 5: SEM micrographs showing bondline of PU+T.

3.2 FTIR Analysis

FTIR spectra of PU with MCC, untreated bark powder, and treated lignocellulose are shown in Figs. S1–S3. It can be observed from the figures that the isocyanate peak at ~2270 cm^{-1} is absent in all spectra, confirming complete curing of the PU adhesive with and without fillers reinforcement. The disappearance of isocyanate peak indicates that the isocyanate groups have fully reacted with polyols and fillers, leaving no residual unreacted NCO functionality. FTIR spectra of unreinforced PU and PU reinforced with MCC (PU+M), PU+UT, and PU+T at 1–5 wt% revealed systematic changes in characteristic absorption bands, confirming enhanced filler–matrix interactions.

PU without filler addition showed typical urethane features with a broad O–H/N–H stretching band between ~3300–3400 cm^{-1}, C–H stretching between ~2850–2970 cm^{-1}, a strong urethane carbonyl band at ~1725 cm^{-1}, and C–O–C/C–O vibrations between ~1000–1150 cm^{-1}. MCC reinforced PU adhesive samples showed broadened O–H/N–H band, while the carbonyl region showed increased contribution from hydrogen bonded urethane C=O (~1705–1710 cm^{-1}) [28]. With increase of MCC content (PU+1M to PU+5M), C–O–C band became narrower and more intense. The sharpening of this peak suggests increased structural order and stronger dipole interactions, likely due to the reinforcement of cellulose into the PU matrix. These changes confirm hydrogen bonding be-tween MCC hydroxyls and PU urethane groups, restricting chain mobility.

PU reinforced with untreated bark powder samples showed similar broadening in the O–H/N–H region and a shift in the carbonyl band. An aromatic skeletal vibration at around ~1510 and ~1600 cm^{-1} is attributed to lignin. This indicates the interfacial bonding between adhesive and the filler [29]. PU reinforced with treated lignocellulose showed several spectral changes. The O–H/N–H band was broadest and most intense, with a clear shifting to longer-wavelength side of the spectrum (~3280–3300 cm^{-1}). This confirms the treated lignocellulose formed strong hydrogen bonds with the PU matrix. The reduced free carbonyl intensity indicates the bonded urethane C=O (~1705 cm^{-1}) in the carbonyl region. The sharper C–O–C bands confirm the improved filler dispersion in the PU matrix. The results demonstrate that surface treatment enhanced the filler–matrix compatibility, producing stronger hydrogen bonding and a more ordered network [30].

The intense absorption band observed in the Fig. 6 Uncured PU sample at 2260 cm^{-1} represents asymmetric stretching vibration of the unreacted isocyanate N=C=O groups. The inset graph highlights a magnified view of the 2400 to 2100 wavenumber region to closely track the chemical changes occurring within this specific isocyanate range. Upon curing, this prominent isocyanate peak sharply disappears in the PU, PU+5M, PU+5UT, and PU+5T spectra. This disappearance of isocyanate peak intensity confirms the successful consumption of isocyanate groups during the polyurethane cross-linking and polymerization process.

The FTIR results show that incorporating the fillers affects the chemical environment of the PU matrix rather than simply causing the disappearance of specific peaks. While the disappearance of the isocyanate (–NCO) band confirms that curing has occurred, systematic band shifts, peak broadening, and intensity changes provide far more compelling evidence of alterations in the local chemical environment. In the MCC-filled PU, hydroxyl groups can form hydrogen bonds with urethane linkages, thereby restricting polymer chain mobility. The lignin-rich UT fillers may interact with the PU through hydrogen bonding and π–π interactions, contributing to the reduction in carbonyl intensity. Among the fillers, treated bark powder appears to produce the strongest interfacial interactions, likely because surface treatment removes extractives and exposes more reactive hydroxyl groups, promoting hydrogen bonding and possible covalent interactions with isocyanate groups. Overall, these spectral changes indicate that curing and filler–matrix interactions are reflected in modifications of the chemical environment rather than being inferred solely from the disappearance of the –NCO peak. These findings suggest that lignocellulosic fillers, particularly treated bark powder, can improve chemical compatibility in PU adhesives.

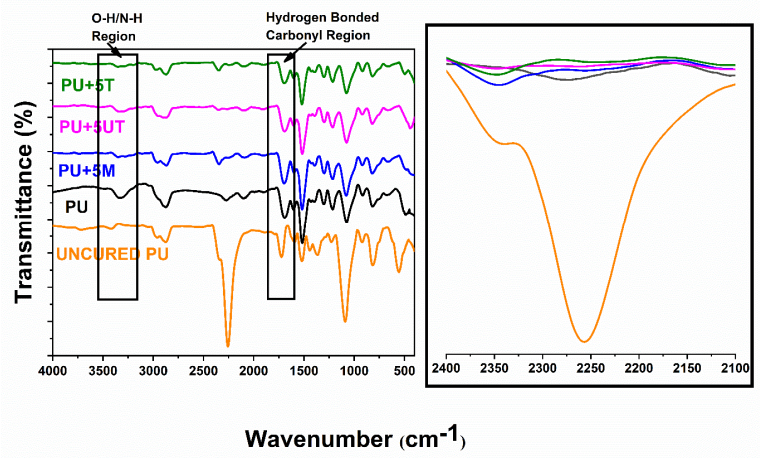

Figure 6: FTIR spectra of uncured PU, unreinforced PU and PU reinforced with MCC, untreated and treated lignocellulose at 5 wt% filler fractions.

3.3 Lap-Shear Strength of the Bonded Joints

Lap-shear strength values of MCC, untreated bark powder and treated lignocellulose reinforced PU adhesive joints are shown in Figs. 7–9, respectively. The lap-shear strength of the joints significantly enhanced due to reinforcement of lignocellulosic fillers compared to the unreinforced PU matrix, which exhibited a baseline strength of 3.05 MPa. For MCC-reinforced PU joints (Fig. 7), lap-shear strength increased with filler content up to 2.5 wt%, reaching a maximum of 4.29 MPa—a 40% improvement over unreinforced PU joints. The increase in strength can be attributed to hydrogen bonding between MCC hydroxyl groups and urethane linkages, which improves interfacial adhesion and stress transfer.

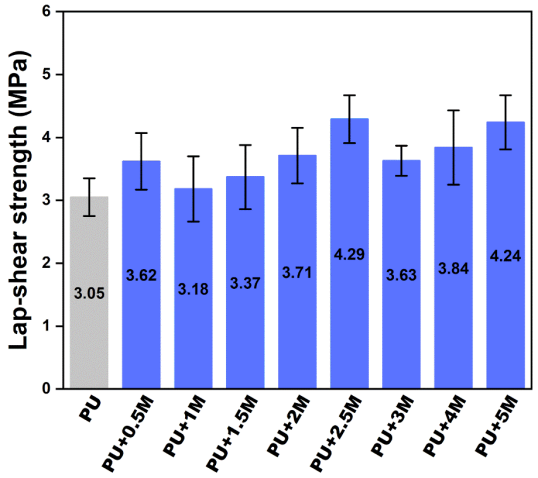

Figure 7: Lap shear test results of unreinforced PU and PU reinforced with MCC at 1–5 wt% filler fractions.

In contrast, PU joints reinforced with UT showed a steady increase in lap-shear strength with increasing filler content (Fig. 8). The lowest strength was recorded for PU+0.5UT (2.74 MPa), while PU+5UT achieved the highest value of 4.31 MPa, representing a 41% increase over unreinforced PU. The increase in strength can be attributed to the presence of lignin in bark powder, whose aromatic structure contributes to mechanical reinforcement, enhancing load-bearing capacity. The gradual increase suggests that UT fillers are more tolerant to higher loadings without compromising matrix integrity.

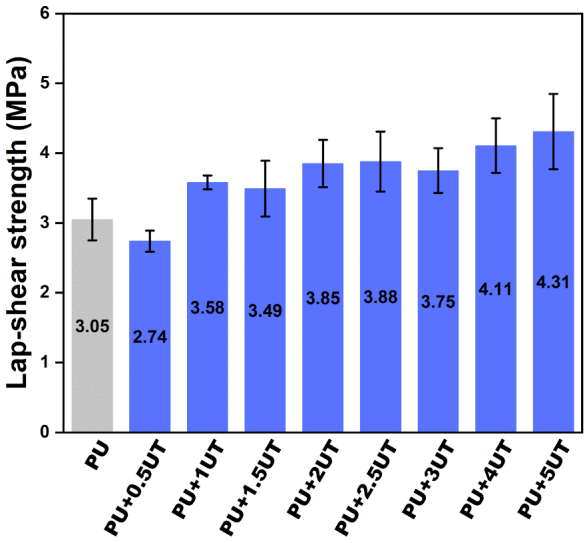

Figure 8: Lap shear test results of unreinforced PU and PU reinforced with UT at 1–5 wt% filler fractions.

PU joints reinforced with T showed the highest lap-shear strength among all joints (Fig. 9), with PU+5T reaching 4.39 MPa—a 44% improvement over unreinforced PU joints. The superior performance can be attributed to the surface treatment, which removes impurities and exposes reactive hydroxyl groups, thereby improving filler–matrix compatibility and promoting stronger hydrogen bonding. This leads to better dispersion, cohesive bonding, and more efficient stress distribution across the joint [17].

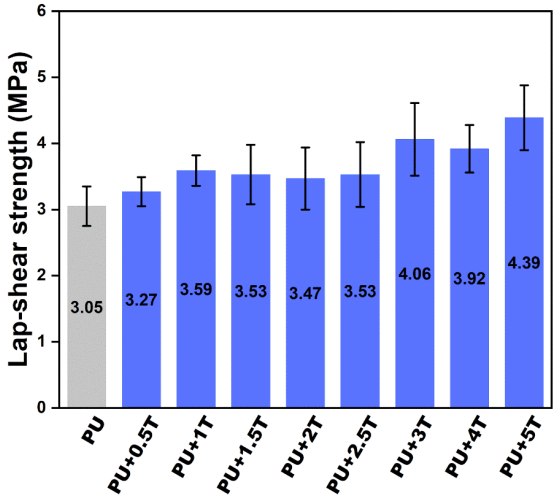

Figure 9: Lap shear test results of unreinforced PU and PU reinforced with treated lignocellulose (T) at 1–5 wt% filler fractions.

A two-way analysis of variance (ANOVA) was conducted to evaluate the effects of filler type, filler concentration, and their interaction on the lap-shear strength of PU adhesive joints. While the main effects of filler type and concentration were not statistically significant (p = 1.00), their interaction had a significant effect on joint strength (F = 1.97, p = 0.013). This indicates that the impact of filler loading influenced joint strength. UT and T lignocellulosic filler-reinforced joints showed distinct trends. Untreated joints showed

only modest gains in lap-shear strength, whereas treated filler addition achieved higher mean strength at specific filler loadings.

Post-hoc comparisons using Tukey's Honestly Significant Difference (HSD) test ($\alpha = 0.05$) revealed not statistically significant pairwise differences between individual groups; all adjusted *p*-values approached 1.0, and 95% confidence intervals crossed zero. As a result, all experimental groups share the same letter grouping "a" (Fig. 10), likely due to high within-group variance. Despite this, the consistent upward trend in mean strength for the treated joints suggests that chemical treatment improved filler–matrix compatibility, leading to better stress transfer across the bond line.

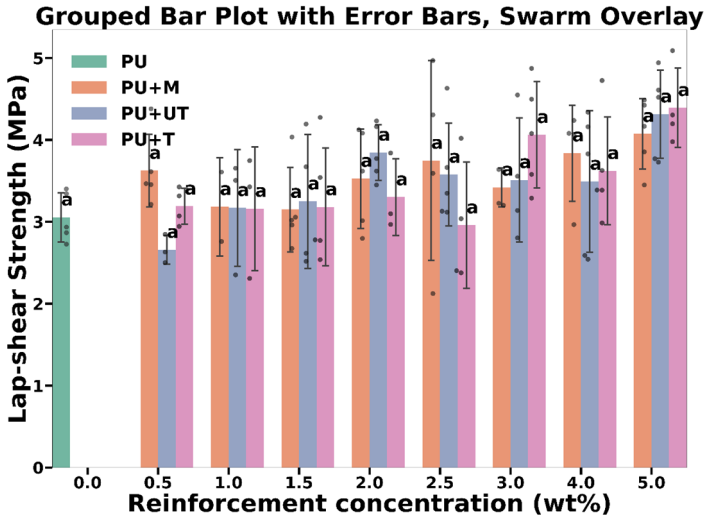

Figure 10: Lap shear strength of unreinforced PU, PU reinforced with MCC, PU reinforced with UT and T lignocellulose at different weight fractions. Bars represent mean ± SD with replicate swarm overlay. Tukey groupings are indicated above each bar; all groups share the same letter ('a').

3.4 Thermogravimetric Analysis

Thermal degradation of MCC, T, and UT powders are shown in Fig. 11a. Below 200°C all samples display a minor, gradual mass loss primarily due to the evaporation of physically bound moisture and low-molecular-weight volatile components. The primary thermal decomposition occurs in the temperature window between 250°C and 400°C, representing degradation of cellulose. For MCC, the degradation of cellulose occurs at 261°C–402°C and for T cellulose degradation occurs between 217°C–374°C while for UT the degradation occurs from 287 to 349°C due to the presence of hemicellulose. A second peak is observed between 460°C–528°C for T and 459°C–530°C for UT due to presence of complex lignin components.

Thermal degradation behaviour of PU without filler addition and PU reinforced with MCC, UT, and T was evaluated to understand filler-matrix interactions and their influence on thermal stability. The TGA/DTG graphs of PU without filler addition and PU reinforced with fillers are shown in Fig. 11b–d and the corresponding temperature values are presented in Table 2. PU without filler addition exhibited decomposition in two distinct stages. First stage degradation corresponds to hard segment at 297°C and second stage degradation of soft segment at 401°C. The urethane bond scission occurred first followed by polyol decomposition and char formation.

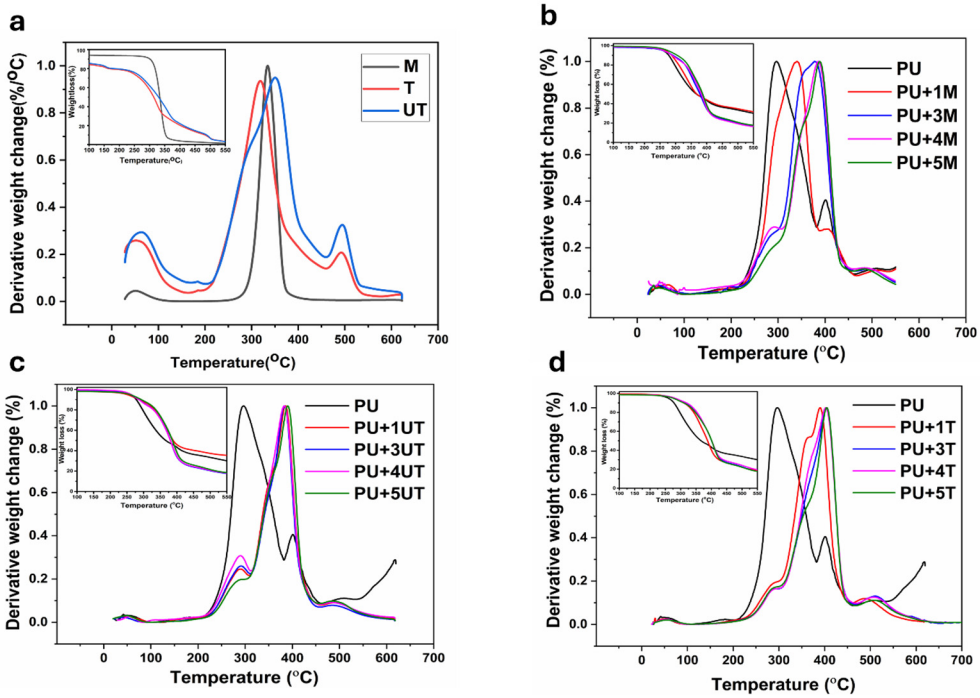

Figure 11: Derivatives of TGA (DTG) and weight loss (inset) curves of (**a**) MCC, UT AND T. (**b**) Unreinforced PU and PU reinforced with MCC at 1–5 wt% filler fractions. (**c**) Unreinforced PU and PU reinforced with UT at 1–5 wt% filler fractions and (**d**) Unreinforced PU and PU reinforced with T at 1–5 wt% filler fractions.

Table 2: Thermal properties of unreinforced and reinforced PU adhesive samples.

Filler Weight Fraction (wt.%)	PU+MCC				PU+UT				PU+T			
	Hard Egments		Soft Segments		Hard Segments		Soft Segments		Hard Segments		Soft Segments	
	Onset (°C)	Peak (°C)	Onset (°C)	Peak (°C)	Onset (°C)	Peak (°C)	Onset (°C)	Peak (°C)	Onset (°C)	Peak (°C)	Onset (°C)	Peak (°C)
0	210	297	389	401	210	297	389	401	210	297	389	401
1	229	341	388	408	302	385	466	486	308	390	404	487
3	306	378	473	491	308	384	469	487	292	404	473	511
4	312	386	469	488	312	383	477	487	290	402	475	510
5	308	389	474	490	308	390	478	488	292	404	478	509

In the case of MCC-reinforced PU adhesive samples, the addition of MCC progressively delayed both thermal degradation stages. The hard segment decomposition shifted from 297°C in neat PU to 341°C for PU+1M, and further increased with filler loading, reaching 389°C at 5 wt%. Similarly, the soft segment degradation moved from 401°C in neat PU to 408°C for PU+1M, with the highest decomposition temperature of 491°C observed at 3 wt%. Beyond this point, a slight decline was noted, with soft segment degradation occurring at 488°C and 490°C for 4 wt% and 5 wt%, respectively. These improvements can be attributed to hydrogen bonding between MCC hydroxyl groups and urethane linkages, which restricts polymer chain mobility and increases the energy required for bond cleavage.

As MCC content increased, DTG peak intensity also increased, and the peaks became sharper. At 3–4 wt%, the DTG profiles were both sharp and symmetric, indicating uniform degradation and optimal filler dispersion. Although the 5 wt% sample exhibited the sharpest and tallest peaks, subtle shoulder formation and baseline broadening were also observed.

In the case of PU reinforced with UT, both degradation stages were progressively delayed compared to neat PU. The hard segment decomposition shifted from 297°C in neat PU to 385°C at 1 wt% and further increased to 390°C at 5 wt%. The soft segment degradation moved from 401°C in neat PU to 486°C at 1 wt%, with a maximum of 488°C observed at 5 wt%. The improvement in stability can be attributed to the presence of lignin's aromatic structure.

DTG profiles showed sharper peaks with increasing UT content. At 3 wt%, the peaks were sharp and symmetric, indicating uniform degradation and effective dispersion. At higher loadings (4–5 wt%), peaks remained sharp but displayed minor irregularities. The increased char yield at higher UT fractions highlights lignin's contribution to thermal stabilization [30].

For PU composites reinforced with T, the most pronounced improvements in thermal stability were observed. Hard segment degradation shifted from 297°C in neat PU to 390°C at 1 wt%, reaching 404°C at 5 wt%. Soft segment decomposition increased from 401°C in neat PU to 487°C at 1 wt%, with the highest value of 511°C recorded at 3 wt%. These shifts represent improvements of more than 100°C compared to neat PU. The enhanced stability can be attributed to surface treatment, which removed impurities and exposed reactive hydroxyl groups, thereby strengthened hydrogen bonding with urethane linkages. This restricts chain mobility and promotes cohesive char formation. DTG peaks at 3–4 wt% were sharp and symmetric, reflecting uniform degradation and optimal dispersion. At 5 wt%, peaks remained sharp and tall, but slight baseline broadening.

From the TGA analysis, it is evident that filler addition delayed thermal degradation. MCC enhanced thermal stability through hydrogen bonding, UT through lignin-derived aromatic stabilization, and treated lignocellulose through a synergistic combination of enhanced interfacial bonding [31].

3.5 Fracture Analysis

The fracture surface analysis provides critical insight into the failure mechanisms governing PU adhesive joints with and without lignocellulosic reinforcement. The observed joint failure modes are: (i) cohesive failure within the adhesive layer, (ii) adhesive (interfacial) failure at the adhesive-substrate interface, and (iii) cohesive failure within the substrate. All the samples of fracture surfaces are presented in Figs. S4–S10. For unreinforced PU joints (Fig. S4), failure was consistently cohesive within the adhesive layer. This mode of failure is typical of polymer adhesives lacking reinforcement, where crack propagation occurs primarily through the adhesive bulk rather than at the substrate interface.

In contrast, the reinforcement of fillers in PU changed the failure modes of joints. These joints failed in 2 ways (i) adhesive (interfacial) failure at the adhesive-substrate interface, and (ii) cohesive failure within the substrate. This high rate of substrate failure proves that the bond between the wood was exceptionally strong.

For MCC reinforced PU adhesive joints (Figs. S5 and S8), fracture surfaces revealed a combination of cohesive failure within the adhesive and the substrate, with high-lighted regions indicating cohesive failure within the substrate. This suggests that hydrogen bonding between MCC hydroxyl groups and urethane linkages enhanced interfacial adhesion sufficiently to shift failure away from the adhesive bulk and into the substrate.

PU joints reinforced with UT displayed similar trends (Figs. S6 and S9). At lower filler fraction (PU+0.5UT), fracture remained largely cohesive within the adhesive, but at higher filler fraction (PU+2.5UT), cohesive failure within the substrate was observed. This transition reflects the reinforcing role of lignin's aromatic structure, which contributes to improved load transfer and mechanical interlocking at the interface. The presence of mixed failure modes confirms that reinforcement of UT fillers enhances joint strength relative to unreinforced PU.

PU joints reinforced with T exhibited the most pronounced improvements (Figs. S7 and S10). Fracture surfaces of PU+T joints showed all three failure modes—cohesive within the adhesive, cohesive within the substrate, and mixed failures—indicating superior interfacial bonding and stress distribution. The surface treatment of lignocellulose likely removed impurities and exposed reactive hydroxyl groups, thereby improving compatibility with the PU matrix. This enhanced filler–matrix interaction explains the higher lap shear strength values observed for PU+T joints and the shift toward substrate failure, the most desirable failure in bonding.

SEM micrographs of fracture surfaces of all the joints are shown in Fig. 12. The shear bands perpendicular to the loading direction were observed across all samples, indicating the characteristic deformation behaviour of PU matrix under shear stress [32]. In the case of reinforced joints, the fillers were uniformly dispersed within the PU matrix with an absence of agglomeration. This is consistent with the lap-shear strength results discussed in earlier Section 3.3. The higher lap-shear strength of reinforced PU joints can thus be attributed to well distributed fillers that enable more efficient stress transfer across the adhesive interface.

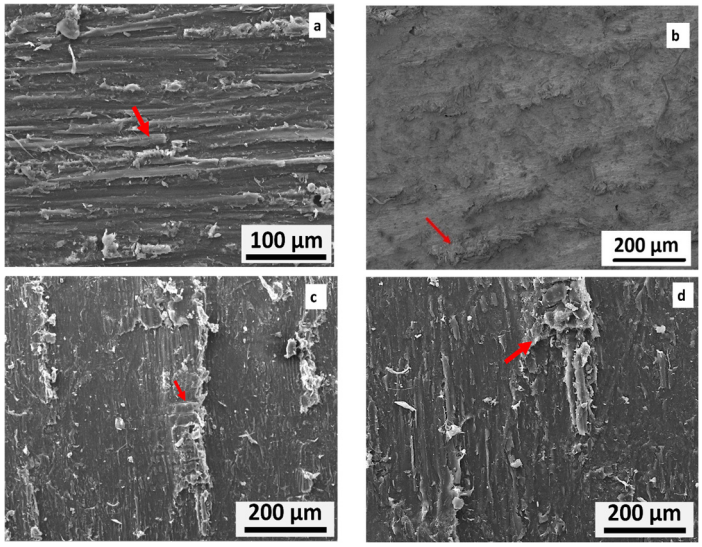

Figure 12: SEM micrographs of fracture surfaces for (**a**) PU, (**b**) PU+MCC, (**c**) PU+UT, and (**d**) PU+T joints.

4 Conclusions

The present study confirmed that the addition of Tamarindus indica bark powder into PU adhesives resulted in a more uniform bondline thickness and reduced the excessive penetration into the substrates.

1. The bathochromic (downward) shift observed in the FTIR spectrum confirms strong interfacial intermolecular hydrogen bonding between the hydroxyl (–OH) groups of the tamarind bark powder and the urethane (–NH) linkages of the PU matrix. This chemical anchoring functions analogously to a micro structured adhesive array, significantly enhancing interfacial adhesion and mechanical

interlocking at the molecular scale. Consequently, this robust interfacial bridge restricts the segmental mobility of the polymer chains during curing, leading to an increase in crosslink density, rigidity, and tensile modulus. Furthermore, the dynamically reversible nature of these hydrogen bonds allows them to act as elastomeric isolators, dissipating mechanical energy under applied stress and impeding crack propagation along the bond line.

2. Lap-shear mechanical evaluation demonstrated that the incorporation of MCC, UT bark powder, and chemically treated lignocellulose significantly enhanced the shear strength of PU adhesive joints relative to the neat PU matrix (3.05 MPa). The MCC-reinforced composite achieved a peak shear strength of 4.29 MPa at an optimal loading of 2.5 wt%, primarily driven by dense intermolecular hydrogen-bonding networks. UT reached 4.31 MPa at 5.0 wt% loading, benefiting from the structural rigidity and non-covalent interactions imparted by lignin's aromatic moieties. The chemically treated bark powder exhibited the highest mechanical performance, attaining 4.39 MPa at 5.0 wt% loading, which highlights the efficacy of surface functionalization in optimizing interfacial compatibility and facilitating efficient stress transfer across the filler-matrix interface.
3. TGA demonstrated a marked enhancement in the thermal stability of the reinforced PU adhesive systems relative to the neat PU matrix. The inclusion of chemically treated lignocellulose significantly retarded thermal degradation, shifting the onset of hard-segment decomposition from 297°C to 404°C. Similarly, the thermal breakdown of the soft segment was delayed from 401°C to 511°C, indicating that surface-functionalized lignocellulosic fillers effectively restrict macromolecular chain mobility and heighten the overall thermal endurance of the polymer matrix.
4. Overall, treated lignocellulose provided the most effective reinforcement, combining uniform bondline morphology, strong interfacial bonding, higher lap-shear strength, and superior thermal stability, thus establishing its potential as an eco-friendly filler for PU adhesives in wood bonding applications.

Acknowledgement: The authors gratefully acknowledge the Science and Engineering Research Board (SERB), Government of India, for providing financial support under the SURE scheme to carry out this research (SUR/2022/003529).

Funding Statement: The authors gratefully acknowledge the Science and Engineering Research Board (SERB), Government of India, for providing financial support under the SURE scheme to carry out this research (SUR/2022/003529) and This work was supported by the Deanship of Scientific Research, Vice Presidency for Graduate Studies and Scientific Research, King Faisal University, Saudi Arabia, Grant No. KFU261868.

Author Contributions: Conceptualization: Lakshmana Rao Bhagavathi, Sk. Gouse and T. Siva; methodology: Lakshmana Rao Bhagavathi, Sk. Gouse and T. Siva; validation: Lakshmana Rao Bhagavathi and Mohammad Faseeulla Khan; formal analysis: Lakshmana Rao Bhagavathi and Mohammad Faseeulla Khan; investigation: Lakshmana Rao Bhagavathi, Sk. Gouse and T. Siva; resources: Lakshmana Rao Bhagavathi, Sk. Gouse and T. Siva; data curation: Lakshmana Rao Bhagavathi and Mohammad Faseeulla Khan; writing—original draft preparation, Lakshmana Rao Bhagavathi, Sk. Gouse and T. Siva; writing—review and editing: Lakshmana Rao Bhagavathi, Mohammad Faseeulla Khan and T. Siva; supervision: Lakshmana Rao Bhagavathi and Mohammad Faseeulla Khan; project administration: Lakshmana Rao Bhagavathi, Sk. Gouse, Mohammad Faseeulla Khan and T. Siva; funding acquisition: Lakshmana Rao Bhagavathi and Mohammad Faseeulla Khan. All authors reviewed and approved the final version of the manuscript.

Availability of Data and Materials: All data that support the findings of this study are included within the article and any Supplementary Files.

Ethics Approval: Not applicable.

Conflicts of Interest: The authors declare no conflicts of interest.

Supplementary Materials: The supplementary material is available online at https://www.techscience.com/doi/10.32604/jpm.2026.088128/s1.

References

1. Otto GP, Moisés MP, Carvalho G, Rinaldi AW, Garcia JC, Radovanovic E, et al. Mechanical properties of a polyurethane hybrid composite with natural lignocellulosic fibers. Compos Part B Eng. 2017;110:459–65. [CrossRef].
2. Wu Q, Henriksson M, Liu X, Berglund LA. A high strength nanocomposite based on microcrystalline cellulose and polyurethane. Biomacromolecules. 2007;8(12):3687–92. [CrossRef].
3. Rueda L, Fernández d'Arlas B, Zhou Q, Berglund LA, Corcuera MA, Mondragon I, et al. Isocyanate-rich cellulose nanocrystals and their selective insertion in elastomeric polyurethane. Compos Sci Technol. 2011;71(16):1953–60. [CrossRef].
4. Lee M, Heo MH, Lee HH, Kim YW, Shin J. Tunable softening and toughening of individualized cellulose nanofibers-polyurethane urea elastomer composites. Carbohydr Polym. 2017;159:125–35. [CrossRef].
5. Saralegi A, Rueda L, Martin L, Arbelaiz A, Eceiza A, Corcuera MA. From elastomeric to rigid polyurethane/cellulose nanocrystal bionanocomposites. Compos Sci Technol. 2013;88:39–47. [CrossRef].
6. Weaver FW, Owen NL. Isocyanate-wood adhesive bond. Appl Spectrosc. 1995;49(2):171–6. [CrossRef].
7. Chen H, Yan N. Application of Western red cedar (*Thuja plicata*) tree bark as a functional filler in pMDI wood adhesives. Ind Crops Prod. 2018;113:1–9. [CrossRef].
8. Pommier R, Elbez G. Finger-jointing green softwood: evaluation of the interaction between polyurethane adhesive and wood. Wood Mater Sci Eng. 2006;1(3–4):127–37. [CrossRef].
9. Lima García J, Pans G, Phanopoulos C. Use of lignin in polyurethane-based structural wood adhesives. J Adhes. 2018;94(10):814–28. [CrossRef].
10. Chen H, Nair SS, Chauhan P, Yan N. Lignin containing cellulose nanofibril application in pMDI wood adhesives for drastically improved gap-filling properties with robust bondline interfaces. Chem Eng J. 2019;360:393–401. [CrossRef].
11. Sharma A, Thakur M, Bhattacharya M, Mandal T, Goswami S. Commercial application of cellulose nanocomposites—a review. Biotechnol Rep. 2019;21:e00316. [CrossRef].
12. Bhagavathi LR, Deshpande AP, Janaki Ram GD, Panigrahi SK. Hygrothermal aging, fatigue and dynamic mechanical behavior of cellulosic particles reinforced one-component moisture curable polyurethane adhesive joints. Int J Adhes Adhes. 2021;105:102771. [CrossRef].
13. Gadhave RV, Kasbe PS, Mahanwar PA, Gadekar PT. Synthesis and characterization of lignin-polyurethane based wood adhesive. Int J Adhes Adhes. 2019;95:102427. [CrossRef].
14. Ajao O, Benali M, Faye A, Li H, Maillard D, Ton-That MT. Multi-product biorefinery system for wood-barks valorization into tannins extracts, lignin-based polyurethane foam and cellulose-based composites: techno-economic evaluation. Ind Crops Prod. 2021;167:113435. [CrossRef].
15. Jin W, Singh K, Zondlo J. Pyrolysis kinetics of physical components of wood and wood-polymers using isoconversion method. Agriculture. 2013;3(1):12–32. [CrossRef].
16. Tenorio-Alfonso A, Sánchez MC, Franco JM. Impact of the processing method on the properties of *Castor* oil/cellulose acetate polyurethane adhesives for bonding wood. Int J Adhes Adhes. 2022;116:103153. [CrossRef].
17. Sozen E, Aydemir D, Zor M. The effects of lignocellulosic fillers on mechanical, morphological and thermal properties of wood polymer composites. Drvna Ind. 2017;68(3):195–204. [CrossRef].
18. Krishnamurthi B, Bharadwaj-Somaskandan S, Sergeeva T, Shutov F. Effect of wood flour fillers on density and mechanical properties of polyurethane foams. Cell Polym. 2003;22(6):371–82. [CrossRef].
19. Pereira RCS, da Silva LRR, Carvalho BA, Mattos ALA, Mazzetto SE, Lomonaco D. Development of bio-based polyurethane wood adhesives from agroindustrial waste. J Polym Environ. 2022;30(5):1959–72. [CrossRef].
20. Abedi-Firoozjah R, Bahramian B, Tavassoli M, Ahmadi N, Noori SMA, Hashemi M, et al. A comprehensive review of gum-based electrospun nanofibers for food packaging: preparation, developments, and potential applications. Int J Biol Macromol. 2025;288:138717. [CrossRef].

21. Zhao F, Xie X, Meng Y, Wang L, Zhu Z, Chen L, et al. Rosin-modified microcrystalline cellulose for enhancing polylactic acid-based composites with good interfacial compatibility and mechanical performance. Polymers. 2026;18(7):889. [CrossRef].
22. Hussin MH, Abd Latif NH, Hamidon TS, Idris NN, Hashim R, Appaturi JN, et al. Latest advancements in high-performance bio-based wood adhesives: a critical review. J Mater Res Technol. 2022;21:3909–46. [CrossRef].
23. Triwulandari E, Fatriasari W, Iswanto AH, Septiyanti M, Umam EF, Ghozali M. Effect of reaction time on the molecular weight distribution of polyurethane modified epoxy and its properties. J Mater Res Technol. 2022;19:2204–14. [CrossRef].
24. Grzybek J, Sepperer T, Petutschnigg A, Schnabel T. Organosolv lignin from European tree bark: influence of bark pretreatment. Materials. 2021;14(24):7774. [CrossRef].
25. Venkatappagari S, Mutra RR, Reddy DM. State-of-the-art in adhesive joint technology: a comprehensive review of recent progress. J Mater Res Technol. 2025;37:2593–615. [CrossRef].
26. Ravichandran B, Balasubramanian M. A comprehensive review on sustainability evaluation of joining methods for engineering materials. Mater Today Sustain. 2025;31:101151. [CrossRef].
27. Srihanam P, Jirum J, Noppawan P, Khotsaeng N, Baimark Y. Preparation and characterization of thermo-compressed guar gum/microcrystalline cellulose composites for applications in sustainable packaging. Polymers. 2025;17(23):3124. [CrossRef].
28. Apaydın Varol E, Mutlu Ü. TGA-FTIR analysis of biomass samples based on the thermal decomposition behavior of hemicellulose, cellulose, and lignin. Energies. 2023;16(9):3674. [CrossRef].
29. Montoya-Escobar N, Ospina-Acero D, Velásquez-Cock JA, Gómez-Hoyos C, Serpa Guerra A, Gañan Rojo PF, et al. Use of Fourier series in X-ray diffraction (XRD) analysis and Fourier-transform infrared spectroscopy (FTIR) for estimation of crystallinity in cellulose from different sources. Polymers. 2022;14(23):5199. [CrossRef].
30. Aristri MA, Sari RK, Lubis MAR, Laksana RPB, Antov P, Iswanto AH, et al. Eco-friendly tannin-based non-isocyanate polyurethane resins for the modification of ramie (*Boehmeria nivea* L.) fibers. Polymers. 2023;15(6):1492. [CrossRef].
31. Raditya VYA, Lubis MAR, Sari RK, Antov P, Lee SH, Kristak L, et al. Properties of ramie (*Boehmeria nivea* (L.) gaudich) fibers impregnated with non-isocyanate polyurethane resins derived from lignin. Materials. 2023;16(16):5704. [CrossRef].
32. Razavi N, Ayatollahi MR, Giv AN, Khoramishad H. Single lap joints bonded with structural adhesives reinforced with a mixture of silica nanoparticles and multi walled carbon nanotubes. Int J Adhes Adhes. 2018;80:76–86. [CrossRef].